SCAPS-1D numerical simulation of homo/heterojunction ZnO/Si solar cells

ABSTRACT

In this article, numerical simulations of the electrical current-voltage characteristics of an n-Si / p-Si homojunction solar cell and an n-ZnO / p-Si heterojunction solar cell are performed. In order to find the optimal structure of the solar cells, numerical modelling using SCAPS-1D (Solar Cell Capacitance Simulator One Dimension) is performed. We study the effect of both emitter and base thicknesses and doping on the cell output parameters which are open circuit voltage (V_{oc}), short circuit current density (J_{cc}), form factor (FF) and conversion efficiency (η). A comparison between the homojunction and heterojunction structures is also made in order to find which one of the two structures has the better conversion efficiency. For the same optimal values of the input parameters, we found that the conversion efficiency of the n-ZnO / p-Si heterojunction (23.23%) is higher than that of the n-Si / p-Si homojunction (20.08%). Therefore, the presence of a transparent conductive oxide (TCO) such as an n-ZnO layer on p-type silicon can improve the conversion efficiency of the solar cell due to the anti-reflection effect of the TCO layer.

Keywords: silicon, zinc oxide, solar cell, homojunction, heterojunction, Scaps-1

1. Introduction

Zinc oxide (ZnO) is a promising semiconductor material for various optoelectronic applications such as thin film solar cell , transparent conducting electrodes , light-emitting diodes (LEDs), due to its large direct bandgap (3.37 eV) and exciton binding energy (60 meV) at room temperature [1]. Due to its high transparency in visible spectrum range and wide direct bandgap, ZnO is a suitable material to be used as a window layer in heterojunction thin film solar cell. Low processing temperature, nontoxicity, abundance, and excellent responsivity in UV region are some additional features of ZnO which can be effectively implemented to improve the fabrication of various optoelectronic devices [2].

The development of technology, for cost reduction and increased performance with respect to the environment, remains challenging. Transparent conducting oxide (TCO) layer on the junction emitter is generally used to enhance the collection of carriers in commercial silicon solar cells. Indium Tin Oxide (ITO), though it has limited source on the earth, is often used as TCO material [3]. Heterojunction solar cell with wide band gap semiconductor emitter layer, namely the zinc oxide (ZnO) layer on silicon absorber has attracted a great deal of interest among researchers in recent times due to its several advantages. Indeed, the processing cost for the deposition of ZnO thin film is low, ZnO is a TCO with good electrical and optical properties and finally it is a non-toxic material [4][5].

Intrinsically, ZnO is an *n*-type semiconductor due to the large number of unintentional defects incorporated and created during the process, with respect to the growth method. These defects are commonly believed to be Zn interstitial and oxygen vacancy. However, *n*-type conductivity of ZnO can be very beneficial to the current Si based thin film solar cell fabrication. Indeed, the emitter of a silicon solar cell is generally fabricated by a high temperature and long diffusion of phosphorus into the bulk silicon to form a pn junction. ZnO layer can be an alternative to the emitter formation by phosphorus diffusion due to its high n-type conductivity as well as antireflection coating effect. This will remove the high temperature diffusion step from the current Si solar cell fabrication process [6][7]. Using ZnO layer over Si provides a window for photon transfer, gives a higher built in potential to increase the open circuit voltage (Voc) and to passive the surface and grain boundary defects, and to reduce the dark current. In addition, in the n-ZnO/p-Si heterojunction solar cells, the solar light (the visible spectrum and near infrared) can be efficiently collected owing to the wide band gap of ZnO (Eg = 3.37 eV).

There are many researches on n-ZnO/p-Si heterojunction solar cells. Hussain et al [8], by simulating an n-ZnO/p-Si solar cell without interface states density, reported a conversion efficiency of about 20 %. Zeng et al [9] fabricated B:ZnO/Si solar cell and reached the following values Voc = 628 mV, Jsc = 41.756 mA .cm $^{-2}$ and efficiency of 17.788 %. The performance of the heterojunction cell strongly depends on the doping concentration, the bulk defect density and the respective thicknesses of n-ZnO and p-Si layers. Indeed, modifying their values affects both charge carrier transport at the junction (recombination and field effects) and photogeneration.

In order to optimize the performance of a solar cell, it is necessary to go through a step of simulation of the solar cell electrical components behavior and to examine the effect of the various manufacturing parameters on the output parameters of the cell. For this purpose, we use the SCAPS1-D (a solar cell

capacitance simulator in one dimension) software for the simulation. We systematically study the effect of emitter and base thicknesses and doping levels on the cell output parameters which are open circuit voltage (Voc), short circuit current density (Jcc), form factor (FF) and conversion efficiency (η) of the n-Si / p-Si homojunction and the n-ZnO / p-Si heterojunction. Then, we make a comparison between the homojunction and heterojunction structure with the aim to emphasize the role the TCO ZnO layer.

2. Methodology

Numerical Modeling has been increasingly used as a tool to understand the physical behavior of the solar cells. Various measurements are done to understand the optical and electrical properties of the solar cell. However, it is difficult to analyze these measurements without a precise model. Therefore, numerical modeling is necessary to interpret the advanced measurement on complicated structures, to design and to optimize advanced cell structures. Following are the most important things to consider in simulation software: capability of solving the basic equations – Poisson equation and the continuity equation for electron and hole [6]. We used the SCAPS software to simulate the current-voltage characteristics of an n-Si/p-Si and n-ZnO/p-Si solar cell with the aim of identifying the optimal manufacturing and operating conditions of these cells.

SCAPS is simulation free software for one-dimensional solar cells developed by the Department of Electronic and Computer Systems of Ghent University, Belgium. SCAPS was originally developed for CuInSe2 and CdTe cell structures. However, several versions have improved its capabilities to become applicable for crystalline solar cells (Si and GaAs) and amorphous cells (a-Si and micro amorphous Si) [10]. With SCAPS, it is possible to simulate structures consisting of a defined number of layers (up to 7 interlayers as well as front and back contacts) with different doping profiles, and with given energy distributions of donor or acceptor levels, in the bulk and at the interfaces for an arbitrary light spectrum [11]. Simulation with SCAPS requires knowledge of the values of a number of physical parameters of the used materials. These parameters are defined in the SCAPS software interface. In the case of the n-Si/p-Si homojunction, the values are presented in Table 1.

Table 1: Physical parameters of silicon introduced in SCAPS[6].

Parameters	Definition	Values
ε_r	Relative Permittivity	11.9
E_g(eV)	Energy gap	1.12
$\chi(eV)$	Electronic affinity	4.05
$N_c(cm^{-3})$	Effective density of states in the conduction band	$2.8\,10^{19}$
$N_V\,(cm^{-3})$	Effective density of states in the valence band	$1.04\,10^{18}$
$\mu_n(cm^2/Vs)$	Electron mobility	1500
$\mu_p(cm^2/Vs)$	Hole mobility	480
V_{the}(cm/s)	Thermal velocity of electrons	10^7
V_{thh}(cm/s)	Thermal velocity of Hole	10^7
T(K)	Temperature	300

Unlike Si, ZnO cannot be used alone in a solar cell because its p-type doping is difficult to achieve and only leads to low hole concentrations. This is due to the combined effects of two properties of ZnO: its

naturally n-type conductivity and its large bandgap. This difficulty in achieving p-type conductivity is general to all large bandgap semiconductors. As a result, ZnO is often combined with other p-type materials such as silicon to form heterojunction. The physical parameters of the heterojunction cell defined in the SCAPS software are presented in Table 2.

Table 2: n-ZnO/p-Si physical parameters introduced in SCAPS [6]**.**

Parameters	**Definition**	**n-ZnO**	**p-si**
ε_r	Relative Permittivity	9	11.9
$E_g(\mathrm{eV})$	Energy gap	3.3	1.12
$\chi(eV)$	Electronic affinity	4.35	4.05
$N_c(cm^{-3})$	Effective density of states in the conduction band	4.410^{18}	$2.8\,10^{19}$
$N_V\,(cm^{-3})$	Effective density of states in the valence band	$7.1\ 10^{19}$	$1.04\ 10^{18}$
$\mu_n(cm^2/Vs)$	Electron mobility	100	1500
$\mu_p(cm^2/Vs)$	Hole mobility	25	480
$V_{the}(cm/s)$	Thermal velocity of electrons	10^7	10^7
$V_{thh}(cm/s)$	Thermal velocity of Hole	10^7	10^7
T(K)	Temperature	300	300

Figure 1 shows the n-Si/p-Si homojunction and n-ZnO/p-Si heterojunction structures that are simulated in this work.

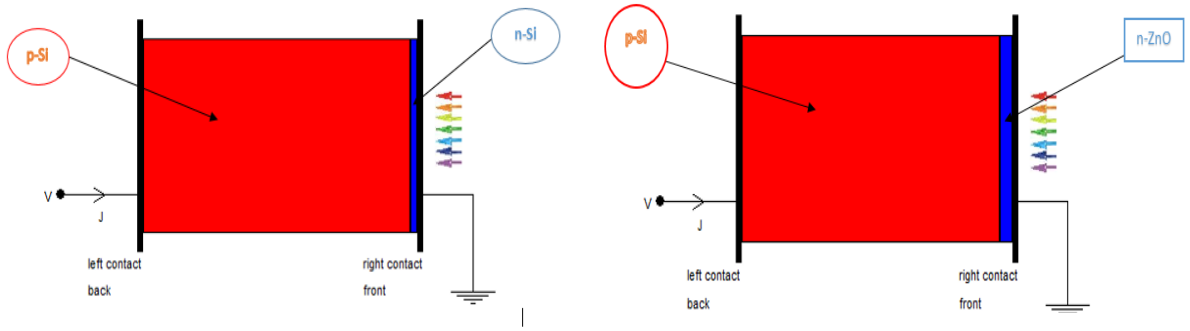

Figure 1: n-Si/p-Si homojunction (left) and n-ZnO/p-Si heterojunction (right) structures in SCAPS

3. RESULTATS AND DISCUSSION

In this section, the simulation results of n-Si/p-Si homojunction and n-ZnO/p-Si heterojunction solar cells are presented. The current-voltage characteristics in dark and under illumination at the 1.5 air mass spectrum (AM) were simulated.

3.1. n-Si/p-Si homojunction solar cell

3.1.1. Current-voltage curve in dark

A typical example of the current-voltage characteristic in dark with SCAPS simulation is represented in **figure 2**. This curve is obtained with the values given in table 1 with an emitter thickness and donor doping density (N_d) of 0.1 µm and 3 10^{18} cm^{-3}, respectively. The collector thickness and acceptor doping density (N_a) are 200 µm and 10^{16} cm^{-3}, respectively. We can notice on this curve that the

current density remains constant for low voltages up to 0.5V, then varies in an exponential way for important values of the voltage (higher than 0.5V). This means that the cell will produce current only for voltages higher than 0.5V in a very efficient way.

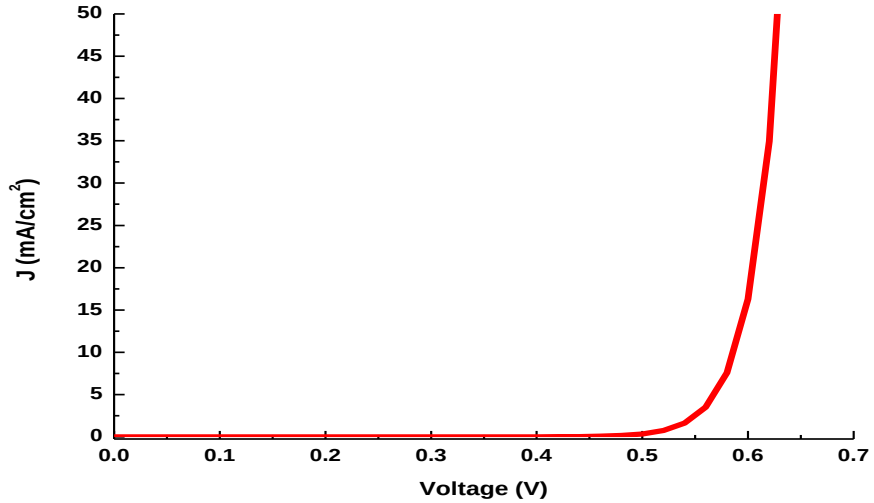

Figure 2: Current-voltage curve in the dark.

3.1.2. Current-voltage curve in darkness and illumination

For the simulation under illumination, the light spectrum we have used is AM1.5G and SCAPS allows automatic loading of the chosen spectrum.

Figure 3 gives the current-voltage characteristics under darkness and under illumination.

The curve under illumination has an offset from the dark curve and this offset corresponds to the photo-current generated (J_{ph}).

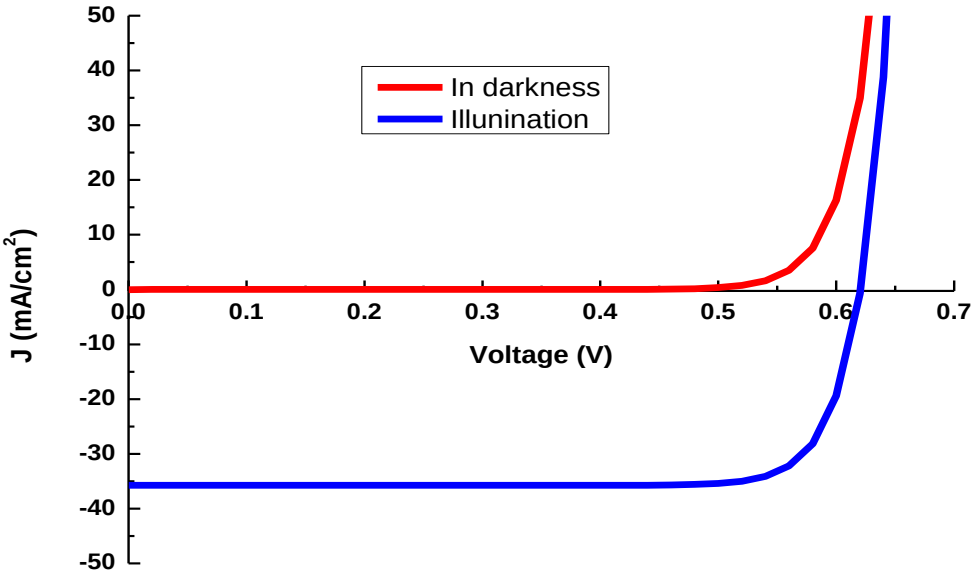

Figure 3: Current-voltage characteristic in darkness and under illumination

3.1.3. Effect of emitter thickness

We have varied the thickness of the emitter from 0.1 to 1µm while keeping constant the other values of table1. The choice of this range of thickness is guided by what it is possible to do experimentally.

The output values of the photovoltaic parameters (V_{oc}, J_{cc}, FF, η) obtained as a function of the emitter thickness are presented in **Figure 4**. With the increase of the emitter thickness, we notice a decrease of the output parameters. Thus V_{oc} and FF slightly decrease from 0.63 to 0.62 V and from 83.06 to 82.86%, respectively. J_{cc} and finally the conversion efficiency also decrease from 44.64 to 27.21mA/cm^2 and from 22.41% to 13.97%, respectively. From these values, we can see that J_{cc} and efficiency η are the two most sensitive parameters to an increase in emitter thickness.

The decrease in photovoltaic parameters can be explained by considering electron-hole pair generations and surface recombinations. Indeed, for small emitter thicknesses, the electron-hole pair generation phenomenon occurs near the interfaces so the surface recombinations increase, which reduces the number of electron-hole pairs. On the other hand, the emitter layer must be as thin as possible to allow the full intensity of the light to pass through. When the thickness of the layer increases, the life span of the minority carriers does not allow them to cross the junction, so they recombine. They no longer have the possibility of crossing the junction to be collected. A thin emitting layer therefore increases the transmitted flux of light. It is concluded that the thinner the layer, the higher the efficiency [12]. However, if the layer is too thin, surface recombination phenomenon increases. A compromise is therefore necessary [13].

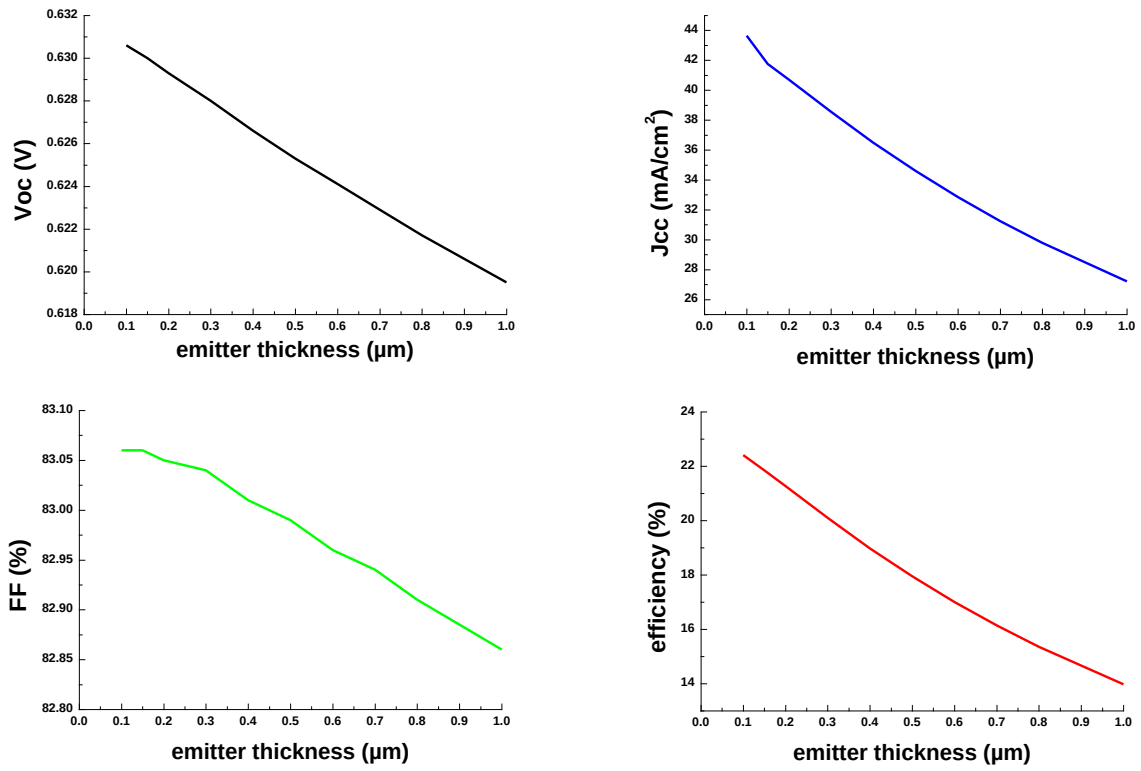

Figure 4: Variation of *Voc* , *Jsc*, , FF and conversion efficiency of the n-Si/p-Si homojunction solar cell with the emitter thickness.

3.1.4 Effect of emitter doping

To study the effect of the cell's emitter doping, we have varied only the donor concentration (N_d) from 10^{16} to 10^{19} cm^{-3}, while keeping the other values given in Table 1 constant. We chose an emitter

thickness of 0.3 µm. **Figure 5** shows the photovoltaic parameter variations as a function of N_d. In this case, a decrease in J_{cc} from 44.65 to 38.52 mA/cm^2 is observed with a change in emitter doping from 10^{16} to 10^{19}cm^{-3}. V_{oc} increases from 0.58 to 0.63 V, FF also shows an increase and finally an increase in conversion efficiency is noticed from 19.54 to 20.11% for the same doping range. We found that the efficiency increases despite the large presence of impurities. These impurities are added to increase the electrical conductivity or to control the carrier lifetime. Therefore, an increase in doping allows an improvement in the conversion efficiency of the structure. Indeed, with the increase in doping, the lifetime of the minority carriers and their mobility increase. On the other hand, as the doping of the emitter layer increases, the potential barrier in the junction increases and the space charge area decreases. The increase in the barrier decreases the diffusion current and increases the photogenerated current. The decrease in the space charge zone results in a decrease of J_{cc} because this current comes from the photogenerated carriers in this zone. The increase in efficiency is related to V_{oc} and FF [12].

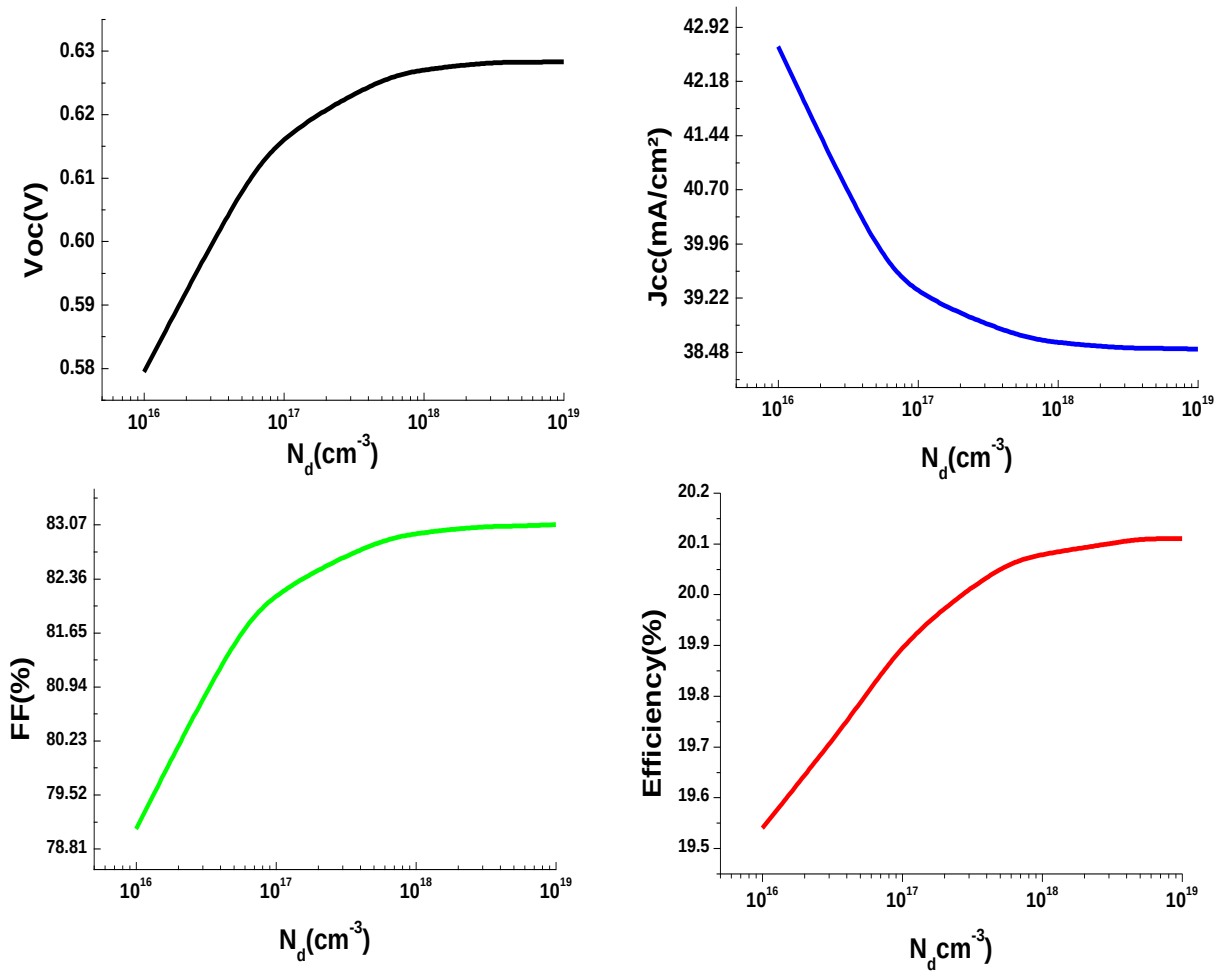

Figure 5: Variation of *Voc* , *Jcc*, , FF and efficiency of the n-Si/p-Si homojunction solar cell as a function of emitter Nd doping

3.1.5 Effect of collector doping

We have also varied the N_a acceptor density of the base from 10^{16} to 10^{18} cm^{-3}. The variations of the photovoltaic parameters (J_{cc}, V_{co}, FF, η) as a function of N_a doping are shown in **Figure 6**.

With the increase of the N_a doping density of the base which constitutes the collector, we notice a small variation of J_{cc}. Indeed, J_{cc} varies from 38.54 to 38.78 mA/cm^2. This small variation is attributed to the narrowing of the width of the depletion zone that occurs in the collector region with the increase in doping density. We also observe an increase in V_{oc}, FF and finally the conversion efficiency of the cell also increases from 20.1 to 23.64%. Indeed, the increase in doping enhances the potential difference between the n and p regions, therefore V_{oc} and FF and the efficiency increase.

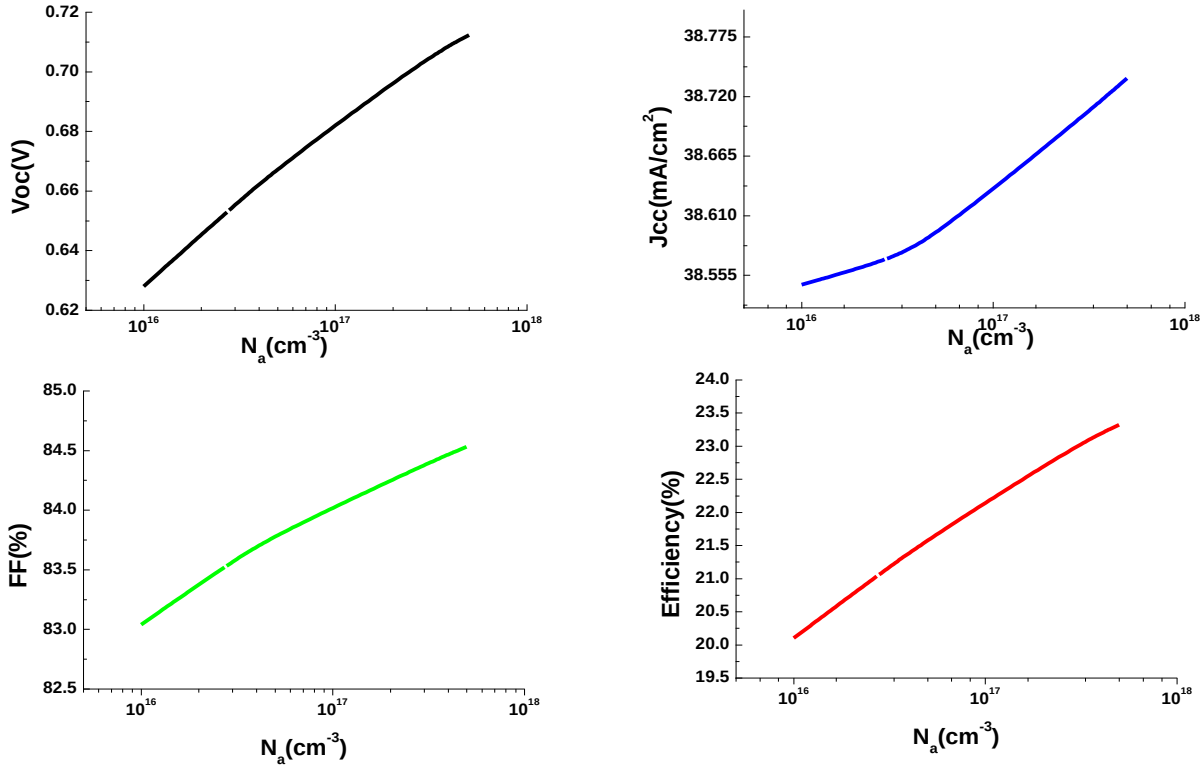

Figure 6: Variation of *Voc, Jcc*, FF and conversion efficiency of the n-Si/p-Si homojunction solar cell as a function of Na doping

3.2. n-ZnO/p-Si heterojunction solar cell

3.2.1 Effect of doping the n-ZnO

In this section, we have studied the effect of the donor doping density (N_d) of the n-ZnO emitter of the heterojunction cell. For this purpose, we have varied the N_d doping concentration from 10^{16} to 10^{19} cm^{-3}, while using the values in Table 2. **Figure 7** represents the variations of the photovoltaic parameters (Jcc, Vco, FF and efficiency) of the heterojunction cell as a function of the N_d doping density of the emitter. Very small variations in the voltage V_{oc} and current J_{cc} are observed with the variation of the emitter doping density. The FF shows an increase and an improvement in conversion efficiency is noticed. This can be explained by the fact that with its high band gap, the ZnO layer allows visible radiation to pass through. This layer is also a transparent conductive oxide and acts as an anti-reflective layer to trap the refracted rays from the silicon reducing the light loss. Thus, the absorption at the silicon is improved and the charged carrier creation is optimized.

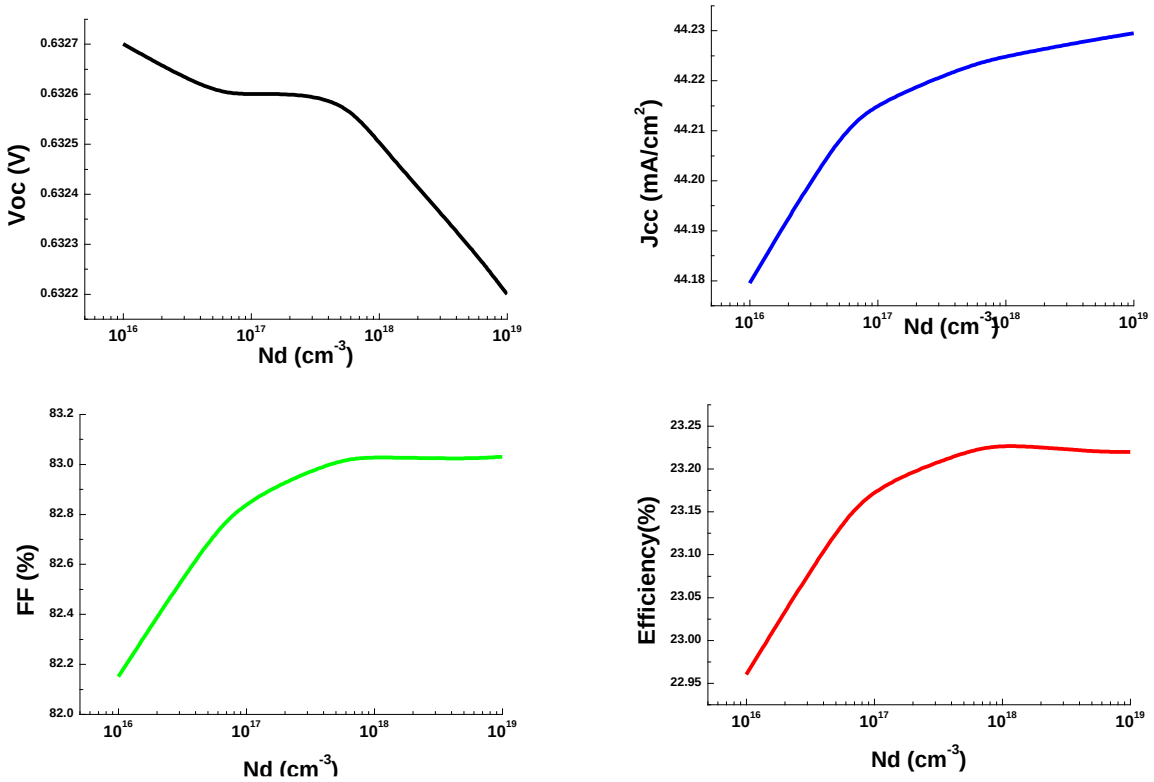

Figure 7: Variation of *Voc* , *Jcc*, , FF and efficiency of the n-ZnO/p-Si heterojunction solar cell as a function of Nd doping density of the n-ZnO layer

3.2.2 Effect of p-Si base doping on the heterojunction

To study the effect of N_a doping density of the base (p-Si layer) of the heterojunction, we have used the values given in Table 2 with a variation of N_a doping density from 10^{16} to 10^{18} cm^{-3}. **Figure 8** shows the variation of the photovoltaic parameters of the heterojunction cell as a function of the N_a doping of the p-Si collector. With the variation of N_a doping density of the p-Si region (which forms the base of the heterojunction) from 10^{16} to 10^{18} cm^{-3}, we observe a small decrease in J_{cc} and an increase in V_{oc}, FF and finally in the efficiency of the n-ZnO/p-Si solar cell from 23.23 to 28.24%. The increase in collector doping density leads to a narrowing of the width of the depletion zone that occurs in the collector region as we have already said. Subsequently the collection of photogenerated carriers will be affected, because it is the internal field of the depletion zone that ensures the dissociation and collection of photogenerated electrons and holes. We have already mentioned that the increase in doping density enhances the potential difference between the n and p regions leading to an increase of Voc, FF and the efficiency.

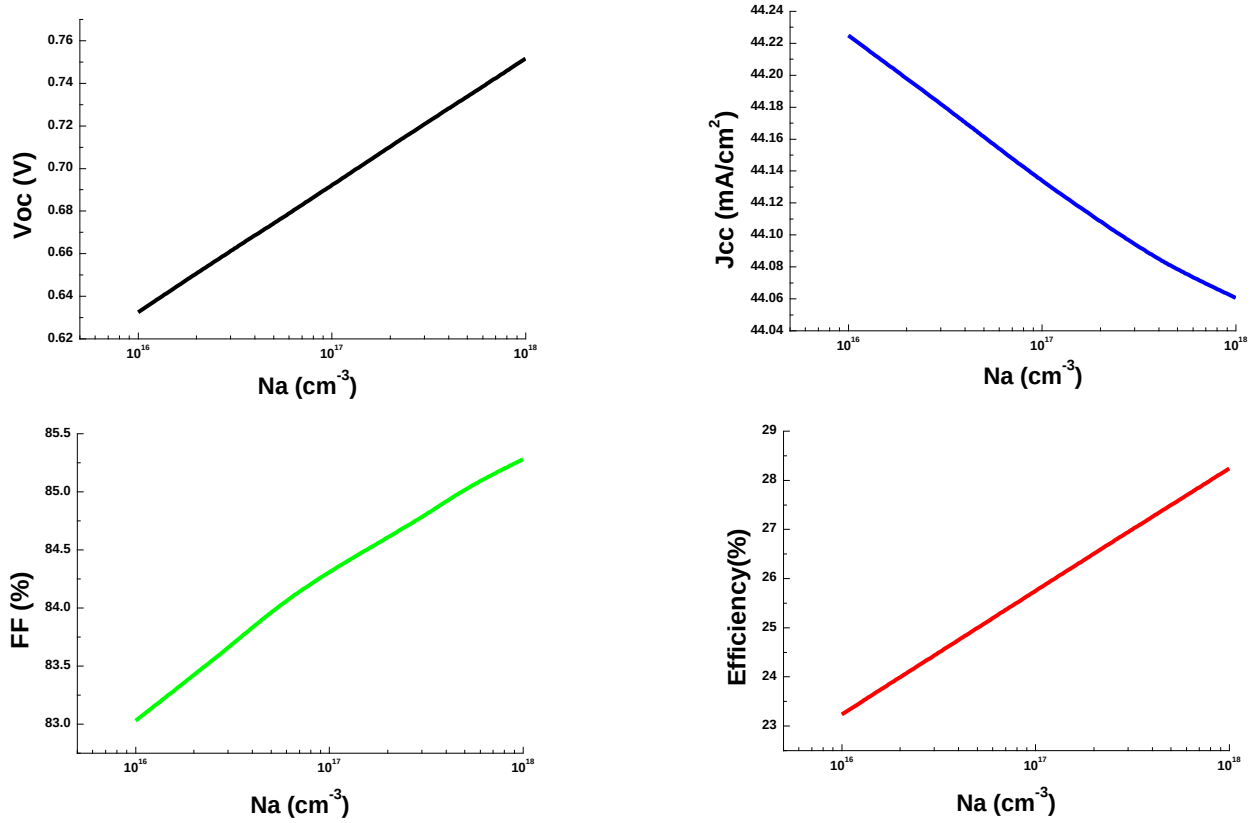

Figure 8: Variation of *Voc* , *Jcc*, , FF and efficiency of the n-ZnO/p-Si heterojunction solar cell as a function of Na doping density of the p-Si collector .

3.3. Comparison between the two structures

With the use of n-ZnO layer as emitter in the n-ZnO/p-Si heterojunction, there is a slight increase in V_{oc}, a significant increase in J_{cc} and almost the same FF and finally an increase in efficiency compared to the electrical parameters (V_{oc}, J_{cc}, FF, efficiency) of the silicon-based np homojunction cell.

3.3.1 Comparison of the effect of emitter doping of the two structures

In this section, we compare the variation of the photovoltaic parameters of our two structures (homojunction and heterojunction) upon the effect of the doping of their respective emitters. **Figure 9** shows that the emitter doping has a much more important effect on V_{oc} and J_{cc} of the homojunction than those of the heterojunction. For FF and efficiency, we observe for both structures practically the same types of variation.

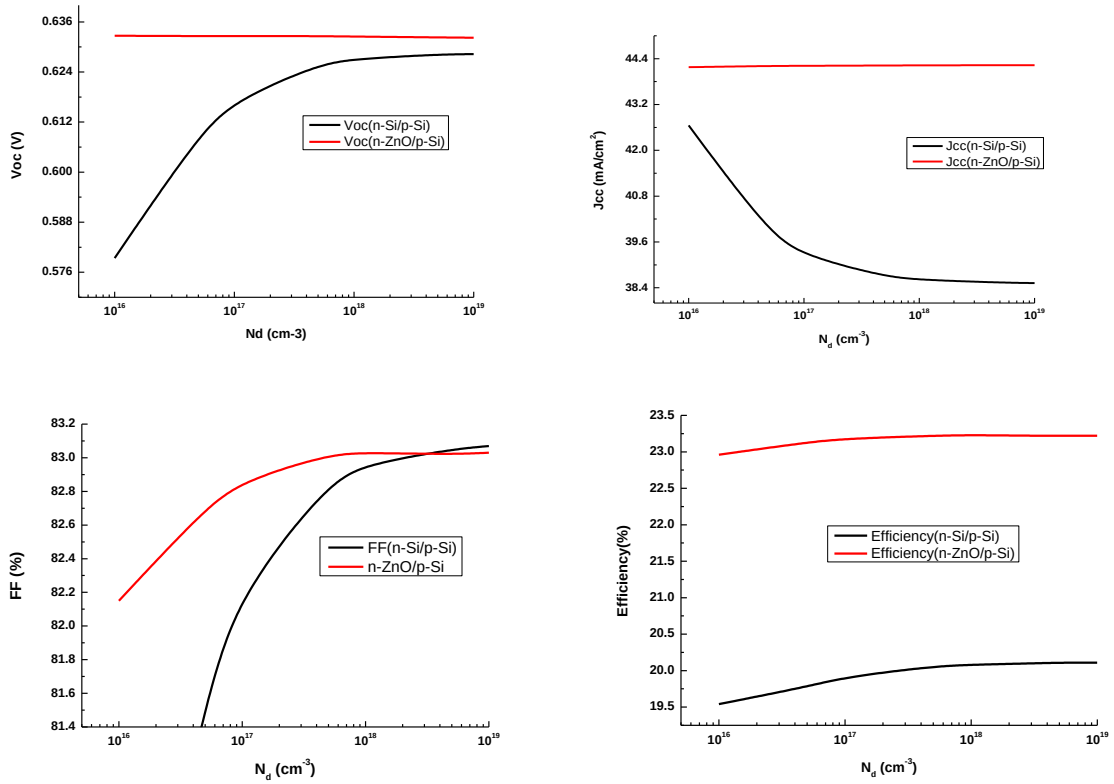

Figure 9 Variation of *Voc* , *Jcc*, , FF and efficiency of two structures(homojunction and heterojunction solar cell) with Nd doping density

3.3.2 Comparison of the effect of doping the base of the two structures

Figure 10 shows the effect of N_a doping on different electrical output parameters of our two structures. It can be seen that with the increase of the base doping of the two structures, the photovoltaic parameters V_{oc}, J_{cc}, FF and the efficiency show the same types of variations.

The observed results of the **figure 9** and **figure 10** show us that the electrical parameters of the heterojunction solar cell are better than those of the silicon based homojunction cell. We can conclude that the performance of the heterojunction is higher than that of the homojunction for given doping density.

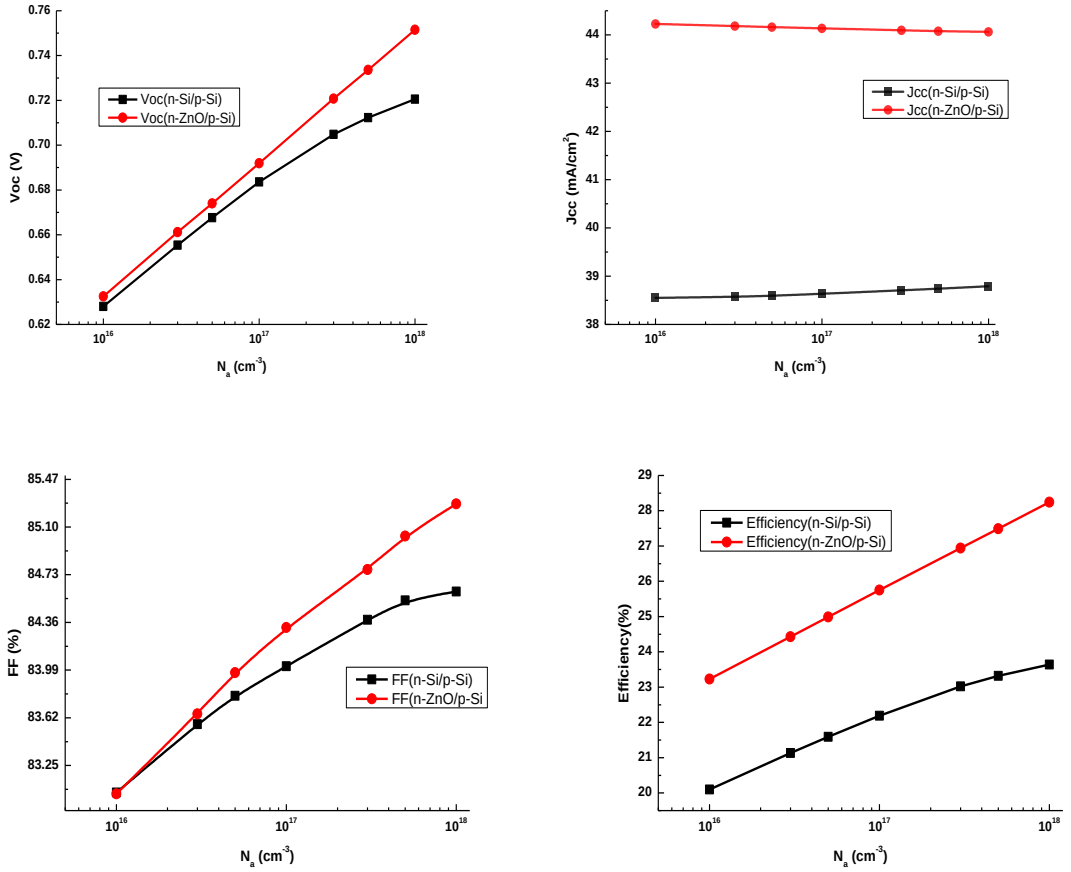

Figure 10: Variation of Voc , Jcc, , FF and efficiency of two structures(homojunction and heterojunction solar cell) with Na doping density.

To illustrate this fact, we summarize in table 3 the obtained photovoltaic parameters of the two structures for an emitter thickness of 0.3 µm, a collector thickness of 200 µm, a doping density of the emitter $N_d = 10^{18}cm^{-3}$ and a doping density of the base $N_a = 10^{16}cm^{-3}$. We observe a conversion efficiency of 23.23% for the heterojunction and 20.08% for the homojunction.

Table 3: Simulated photovoltaic parameters of the two structures (homojunction and heterojunction)

Structure	Voc (V)	Jsc (mA/cm²)	FF (%)	Efficiency (%)
n-Si/p-Si	0.6271	38.61	82.96	20.08
n-ZnO/ p-Si	0.6325	44.23	83.03	23.23

Our results are comparable the simulated values of Hussain et al [8] who reported Voc, Jsc, FF and conversion efficiency values of 0.662 V, 37.7 mA/cm², 81.5% and 20.34%, respectively for n-ZnO/ p-Si hetrojunction. In addition, for the validation of our simulated results, we use the experimental results in references [7] [9]. We find a good agreement. Indeed, Yusupov et al [7] reported Voc, Jsc, FF and conversion efficiency values of 0.68 V, 39 mA/cm², 82% and 21%, respectively for n-ZnO/ p-Si hetrojunction. Whereas Zeng et al [9] fabricated B:ZnO/Si solar cell and reached the following values

Voc = 0.628 V, Jsc = 41.756mA .cm $^{-2}$ and efficiency of 17.788 %. The slight differences between the simulated results and the experimental one are due to the real condition of the experiment. In the simulation, the ideal structures are considered that is all dopant atoms are assumed to be electrically active; there are no defects in the structures for example. All these parameters can affect the actual conversion efficiency.

4. CONCLUSION

In this study, we have performed numerical simulations of the electrical current-voltage characteristics of an n-Si / p-Si homojunction and an n-ZnO / p-Si heterojunction solar cells. We have examined the effect of both the solar cell emitter and base doping and thickness on the output parameters such as V_{oc}, J_{cc}, FF and conversion efficiency. We find that the n-Si/p-Si cell homojunction solar presents an efficiency of 20.08%, for an emitter of 0.3 µm thickness and doping of 10^{18} cm^{-3} and a base of 200 µm thickness with a doping of 10^{16} cm^{-3}. Whereas, for the heterojunction structure, we obtain an efficiency of 23.23% with the same parameters that is 0.3 µm thick emitter with a doping of 10^{18} cm^{-3} and a base of 200 µm with a doping of 10^{16} cm^{-3}. Therefore, heterojunction solar cell shows a higher performance compared to the n-Si/p-Si cell. This is due to the transparent conductive oxide character of ZnO which acts as an anti-reflection layer thus trapping the refracted rays from the silicon reducing the light loss. This leads to an improvement of the light absorption in the silicon increasing the electron-hole pair generation.

DISCLAIMER (ARTIFICIAL INTELLIGENCE)

Author(s) hereby declare that NO generative AI technologies such as Large Language Models (ChatGPT, COPILOT, etc.) and text-to-image generators have been used during the writing or editing of this manuscript.

AKNOWLEDGEMENTS

We gratefully acknowledge Dr. Marc Burgelman at Gent University, Belgium, for providing the opportunity to use SCAPS-1D simulation software.

COMPETING INTERESTS

Authors have declared that no competing interests exists

REFERENCES

[1] F. Z. Bedia, A. Bedia, B. Benyoucef, and S. Hamzaoui, (2014), “Electrical characterization of n-ZnO/p-Si heterojunction prepared by spray pyrolysis technique,” *Phys Procedia*, vol. 55, pp. 61–67, doi: 10.1016/j.phpro.2014.07.010.

[2] L. Mandal, S. S. A. Askari, and M. Kumar,(2019) “Analysis of ZnO / Si Heterojunction Solar Cell with Interface Defect Analysis of ZnO / Si Heterojunction Solar Cell with Interface Defect,” in *U. Biswas et al. (eds.), Advances Advances in Computer, Communication and Control . Lecture Notes in Networks and Systems, vol 41.*, Springer Singapore,. doi: 10.1007/978-981-13-3122-0.

[3] S. Ullah, A. Gulnaz, and G. Wang, “Modeling and Simulation of Heterojunction Solar Cell with Mono Crystalline Silicon,” *Journal of Applied Mathematics and Physics*, vol. 12, no. 03, pp. 997–1020, 2024, doi: 10.4236/jamp.2024.123061.

[4] S. Sadique, A. Askari, M. Kumar, and M. K. Das, “Numerical study on the interface properties of a ZnO / c-Si heterojunction solar cell,” *Semicond Sci Technol*, vol. 33, no. 11, p. 115003, 2019, doi: 10.1088/1361-6641/aadf71.

[5] P. Luppina, P. Lugli and S. M. Goodnick, "Modeling of silicon heterojunction solar cells," *2015 IEEE 42nd Photovoltaic Specialist Conference (PVSC)*, New Orleans, LA, USA, 2015, pp. 1-6, doi: 10.1109/PVSC.2015.7356049.

[6] M. S. B. N. Ziani,(2018) “Computer Modeling Zinc Oxide/Silicon Heterojunction Solar Cells,” *JOURNAL OF NANO- AND ELECTRONIC PHYSIC*, vol. 10, no. 6, pp. 6–11, doi: 10.21272/jnep.10(6).06002.

[7] F. T. Yusupov, T. I. Rakhmonov, M. F. Akhmadjonov, M. M. Madrahimov, and S. S. Abdullayev,(2024) “ENHANCING ZnO/Si HETEROJUNCTION SOLAR CELLS: A COMBINED EXPERIMENTAL AND SIMULATION APPROACH1,” *East European Journal of Physics*, vol. no. 3, pp. 425–434, 2024, doi: 10.26565/2312-4334-2024-3-51.

[8] B. Hussain, A. Ebong, and I. Ferguson, “Zinc oxide as an active n-layer and antireflection coating for silicon based heterojunction solar cell (2015),” *Solar Energy Materials and Solar Cells*, vol. 139, pp. 95–100 , doi: 10.1016/j.solmat.2015.03.017.

[9] Xiangbin Zeng, Xixing Wen, Xiaohu Sun, Wugang Liao, Yangyang Wen, Boron-doped zinc oxide thin films grown by metal organic chemical vapor deposition for bifacial a-Si:H/c-Si heterojunction solar cells, Thin Solid Films, Volume 605, 2016, Pages 257-262, https://doi.org/10.1016/j.tsf.2015.11.023.

[10] M. Burgelman and K. Decock, *Marc Burgelman, Koen Decock, Alex Niemegeers, Johan Verschraegen, Stefaan(*,version, 2016*)‘Manuel SCAPS.’”* Université de Gent.

[11] S. Khelifi and A. Belghachi, (2004)“Le Rôle de la Couche Fenêtre dans les Performances d ’ une Cellule Solaire GaAs,”’” *Rev . Energ . Ren*, vol. 7, pp. 13–21.

[12] H. Mathieu and H. Fanet, *“‘Physique des semiconducteurs et des composants électroniques,’”* 6e édition. 2009.

[13] W. L. Rahal and D. Rached,(2018) “ Optimisation De L’Emetteur Des Cellules Solaires A Hétérojonction De Silicium,”. 5 ème Séminaire International sur les Energies Nouvelles et Renouvelables: https://www.researchgate.net/publication/328582681